J Solid State Electrochem (2003) 7: 665–670
DOI 10.1007/s10008-003-0368-x

ORIGINAL PAPER

E. S. Ribeiro · S. S. Rosatto
Y. Gushikem · L. T. Kubota

Electrochemical study of Meldola's blue, methylene blue and toluidine blue immobilized on a SiO_2/Sb_2O3 binary oxide matrix obtained by the sol-gel processing method

Received: 29 October 2002 / Accepted: 14 February 2003 / Published online: 29 March 2003

Abstract SiO_2/Sb_2O_3 (SiSb), having a specific surface area, S_{BET}, of 788 $m^2\ g^{-1}$, an average pore diameter of 1.9 nm and 4.7 wt% of Sb, was prepared by the sol-gel processing method. Meldola's blue (MeB), methylene blue (MB) and toluidine blue (TB) were immobilized on SiSb by an ion exchange reaction. The amounts of the dyes bonded to the substrate surface were 12.49, 14.26 and 22.78 μmol g^{-1} for MeB, MB and TB, respectively. These materials were used to modify carbon paste electrodes. The midpoint potentials (E_m) of the immobilized dyes were −0.059, −0.17 and −0.18 V vs. SCE for SiSb/MeB, SiSb/MB and SiSb/TB modified carbon paste electrodes, respectively. A solution pH between 3 and 7 practically did not affect the midpoint potential of the immobilized dyes. The electrodes presented reproducible responses and were chemically stable under various oxidation-reduction cycles. Among the immobilized dyes, MeB was the most efficient to mediate the electron transfer for NADH oxidation in aqueous solution at pH 7. In this case, amperometric detection of NADH at an applied potential of 0 mV vs. SCE gives linear responses over the concentration range of 0.1–0.6 mmol L^{-1}, with a detection limit of 7 μmol L^{-1}.

Keywords Chronoamperometry · NADH · Redox dyes · SiO_2/Sb_2O_3 mixed oxide · Sol gel

Introduction

The binary oxides SiO_2/M_xOy obtained by the sol-gel processing method have found many applications in recent years [1, 2, 3, 4, 5, 6, 7, 8, 9]. The materials obtained have combined the mechanical properties of the silica matrix with the chemical properties of the bulk metal oxides. The sol-gel process permits obtaining a solid with controlled porosity and the metal oxide can be obtained as highly dispersed particles in the matrices [8]. Basically, the procedure consists of a reaction between the reagents tetraethyl orthosilicate, $Si(OEt)_4$, and the metal oxide precursor, $M(OR')_4$:

$$Si(OEt)_4 + xM(OR')_y \xrightarrow{\text{solv + acid}} SiO_2/M_xO_y + 4EtOH + xyR'OH \quad (1)$$

The growing interest in using these materials as a porous substrate to immobilize electroactive species is the possibility to prepare a series of electrochemical sensors (chemically modified electrodes) [1, 2, 10, 11, 12, 13].

Studies have demonstrated that Meldola's blue (MeB) and toluidine blue (TB) can be immobilized on a SiO_2 matrix grafted with TiO_2 and, furthermore, used to prepare modified carbon paste electrodes for use as electrochemical sensors for NADH [14] or oxalate ion [15]. Methylene blue (MB) and MeB have also been immobilized on bulk zirconium phosphate [16, 17], on silica-titanium phosphate [13] or on silica-zirconia-antimonia [2] prepared by the sol-gel processing method. In these three cases the main characteristic was that modified carbon paste electrodes made with the materials with immobilized dyes, immersed in solutions with a wide range of pH, showed a constant midpoint potential, in contrast to those observed for the dyes in the solution phase [18] or when immobilized on a graphite surface [19, 20]. The shift of E_m toward more positive values is desirable to enhance the redox reaction between NADH and mediator, resulting in more efficient electrocatalysis [21].

Antimony(III) oxide has been used in numerous applications: as a flame retardant [22, 23, 24, 25], as the main component for glass formation [26], as a catalyst [27, 28, 29, 30] and as an ion exchanger [31, 32]. Within these applications, its use as an ion exchanger is of

E. S. Ribeiro · S. S. Rosatto · Y. Gushikem (✉)
L. T. Kubota
Instituto de Quimica, UNICAMP,
Caixa Postal 6154, 13084-862
Campinas, SP, Brazil
E-mail: gushikem@iqm.unicamp.br
Fax: +55-19-37883023

particular interest. However, the oxide as the substrate base to adsorb electroactive species presents limitations because the powder obtained shows a low mechanical resistance. To increase such mechanical resistance the mixed oxide SiO_2/Sb_2O_3, prepared by the sol-gel method, was used as the substrate base to adsorb, by an ion exchange reaction, MeB, MB and TB.

Electrochemical studies of the immobilized dyes fixed on a porous matrix surface, aimed at developing an electrode presenting high sensitivity and chemical stability, are described in this work. The electrodes made with the material were tested in the electron-mediated process for NADH electrooxidation.

Experimental

Preparation of SiO_2/Sb_2O_3 mixed oxide

The mixed oxide SiO_2/Sb_2O_3, hereafter designated as SiSb, was prepared according to the following procedure. To 210 mL of a 50% (v/v) solution of ethanol/TEOS (TEOS = tetraethyl orthosilicate) were added 12 mL of 3.5 mol L^{-1} HCl. The mixture was stirred for 3 h at 330 K. After the pre-hydrolysis step, 22 g of $SbCl_3$ was added and the mixture stirred for 3 h at room temperature. An additional 6.0 mL of 3.5 mol L^{-1} HCl solution was added and the mixture stirred for 2 h more at room temperature. The solvent was slowly evaporated at 333 K until gel formation. The gel obtained was ground and sieved between 60 and 200 mesh and the resulting particles washed with ethanol in a Soxhlet extractor for 8 h. Finally, the material was washed with 250 mL of 0.1 mol L^{-1} HNO_3, bidistilled water, dried under vacuum (1.3×10^{-2} Pa) and stored.

Scanning electron microscopy

A JEOL JSM T300 scanning electron microscope (SEM), equipped with an energy dispersive (EDS) microprobe from NORAN Instruments, model series 2, was used to obtain the micrographs of the material. The samples were dispersed on double-faced conductive tape on a copper support and coated with gold using BALZER MED 020 equipment.

Specific surface area and chemical analysis of SiSb

The specific surface area, S_{BET}, and the average pore diameter were measured by the BET multipoint technique on a Micromeritics model ASAP 2010 apparatus. The antimony content in SiSb was determined by using X-ray fluorescence analysis on a model 5000 spectrometer equipped with beryllium window (Tracor X-Ray).

Dye immobilization on SiSb

MeB, MB and TB (Fig. 1) were adsorbed on the SiSb matrix from a solution phase. About 0.5 g of SiSb was immersed in 50 mL of the dye solution, with dye concentrations between 4.0×10^{-5} and 1.0×10^{-3} mol L^{-1}. The mixtures were shaken for 30 min, the time required for the system to achieve equilibrium. The change of the dye concentrations in the solution phase, before and after equilibrium, was measured by spectrophotometry and the amount of incorporated dye, N_f, in the matrices was determined by applying the equation: $N_f = (N_a - N_s)/m$, where N_a and N_s are the initial and final (equilibrium) mole numbers of the dye in the solution phase, respectively, and m is the mass of the material. The materials obtained, SiO_2/Sb_2O_3/MeB, SiO_2/Sb_2O_3/MB and SiO_2/Sb_2O_3/TB, will be hereafter designated as SiSb/MeB, SiSb/MB and SiSb/TB, respectively.

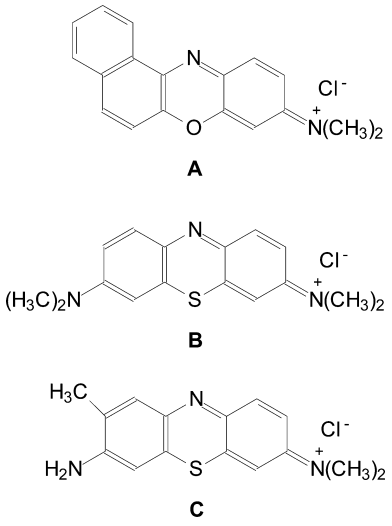

Fig. 1 Structural formulae of the dyes studied: **A** Meldola's blue, **B** methylene blue and **C** toluidine blue

UV-visible spectra of the dyes on SiSb

The UV-visible spectra of the solid samples were obtained as a mull in hydrocarbon oil between quartz plates with a 0.1 mm path length. The measurements were carried out on a Beckman DU 640 spectrophotometer.

Electrochemical measurements

All the measurements were carried out under a pure nitrogen atmosphere in a cell with three electrodes: saturated calomel (SCE) as the reference electrode, platinum wire as the counter electrode and a modified carbon paste electrode as the working electrode. The modified carbon paste electrode was prepared by mixing 30 mg of graphite and 30 mg of binary oxide containing the immobilized dye (SiSb/dye) with hydrocarbon oil as the binder. The measurements were performed on a PAR model 273 A (EG&G) potentiostat-galvanostat apparatus. The supporting electrolyte used in the experiments was 0.2 mol L^{-1} KCl and the solution pH was adjusted through additions of HCl or KOH.

The electrocatalytic properties for NADH oxidation of the SiSb/dye-modified carbon paste electrodes were investigated by cyclic voltammetry and amperometry using additions of freshly prepared NADH solution in a 0.06 mol L^{-1} phosphate buffer solution containing 0.2 mol L^{-1} KCl solution.

Results and discussion

Characterization of the materials

The SiSb binary oxide prepared by the sol-gel method resulted in a highly porous material with a specific surface area, S_{BET}, of 788 m^2 g^{-1} and an average pore diameter of 1.9 nm. The amount of Sb incorporated in the binary oxide was 4.7 wt% (0.39 mmol g^{-1}).

Figure 2 show the EDS Sb mapping image obtained for the SiSb material. The white points in Fig. 2 are due to the antimony L_α radiation energy at 3.6 keV [33, 34]. It can be observed from the EDS image that the Sb atoms are, within the magnification used, uniformly dispersed without any detectable islands of the oxide particles in the matrix. This homogeneous dispersion of the metal oxide in the matrix is an important characteristic for applications of the material.

The amounts of the dyes immobilized on the matrix are presented in Table 1.

Molecular associations of the dyes

Since the dyes can form molecular associations, normally as dimers and sometimes as higher order aggregates, in the solution phase [35, 36] and since such behavior could persist in the solid phase, SiSb/dye with different dye loadings was obtained. The reason is that the redox potential can be affected by the nature of aggregation of the dyes in the solid matrices. Figure 3 show the spectra in the solid phase obtained for SiSb/MB with different dye loadings and the spectra were compared with MB in aqueous solution. The peak at the lower wavelength, ~610 nm, is due to the dimeric species and at the higher wavelength, ~660 nm, is due to the monomeric species [36, 37]. Estimations of the relative amounts of both species by determining the band areas under the deconvoluted peaks were made and the results obtained are listed in Table 1. It is clearly observed that the monomeric species predominated in more dilute dyes. This effect may affect the electrochemical behavior of the dyes.

Table 1 also lists the results obtained for SiSb/MeB and SiSb/TB, following similar procedures. The spectra of these last two solids are not shown because they are similar to that of SiSb/MB.

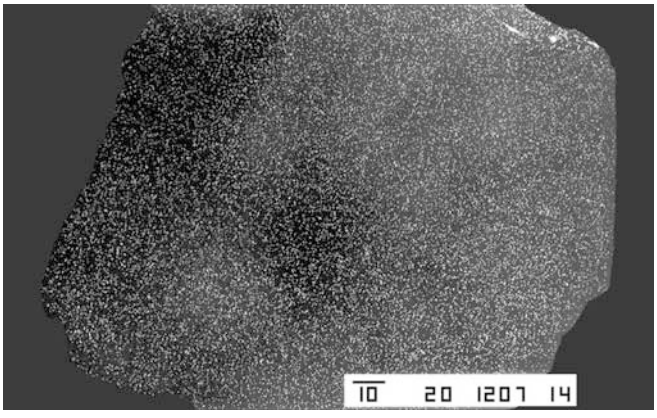

Fig. 2 Energy dispersive scanning image (EDS) of antimony. *Bars* indicate 10 μm

Table 1 Amounts of the dyes immobilized on SiSB, E_m values and the dimeric/monomeric ratio

SiSb/dye	Amount (μmol g^{-1})	E_m (mV vs. SCE)	Dimeric/monomeric ratio[a]
SiSb/MeB	33.4	−80	2.0
	12.5	−59	1.3
	3.6	−53	0.9
SiSb/MB	35.1	−185	1.3
	14.3	−172	0.8
	3.6	−102	0.5
SiSb/TB	22.8	−189	2.3
	13.7	−184	1.2
	3.5	−138	0.6

[a]Dimeric/monomeric ratio = d/m

Electrochemical studies

As discussed above, the dyes adsorbed on the matrix show the same tendencies to associate as dimeric or higher order species as observed in the solution phase. As a consequence, the midpoint potential E_m [$E_m = (E_a + E_c)/2$, where E_a and E_c are the anodic and cathodic peak potentials] is also affected by this tendency for association. It is clearly observed by the data listed in Table 1 that in every case E_m values become more positive as the dimeric/monomeric ratios (d/m) decrease. This behavior may affect the electrocatalytic

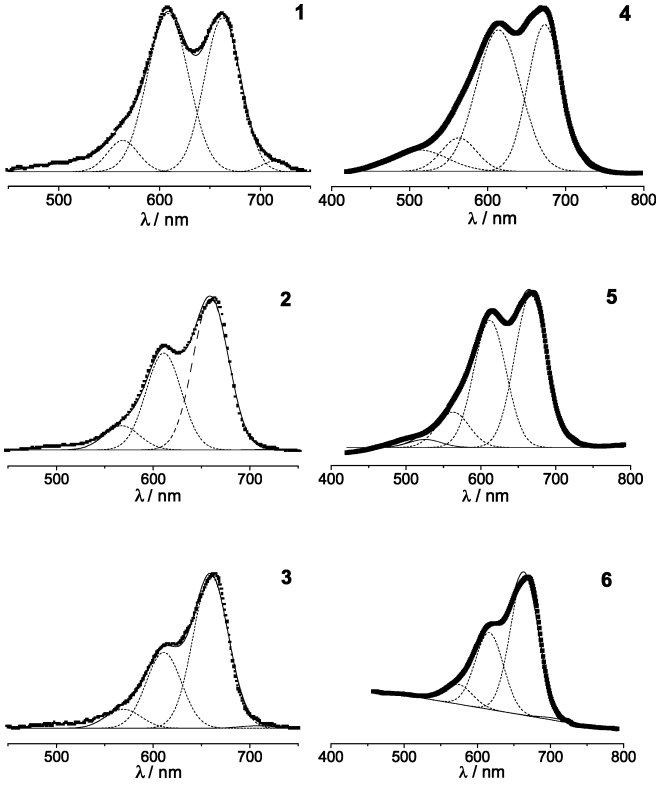

Fig. 3 UV-vis absorption spectra of MB in aqueous solution (**1**, 2.0×10^{-4}; **2**, 5.0×10^{-5}; **3**, 1.25×10^{-5} mol L^{-1}) and of SiSb/MB with different amounts of adsorbed methylene blue (**4**, 35.2; **5**, 14.3; **6**, 3.6 μmol g^{-1})

activity, since the thermodynamic driving force of the reaction can be increased.

Figure 4 shows the cyclic voltammograms of the modified carbon paste electrode of SiSb/MB, for various dye loadings in the matrices, obtained in 0.5 mol L^{-1} supporting electrolyte solution at a scan rate of 20 mV s^{-1}. Sweeping the potential between −0.4 and 0.3 V, no peak currents for the SiSb-modified carbon paste electrode (Fig. 4a) are observed. For the MB adsorbed solid modified carbon paste electrode (Fig. 4b–d), well-defined anodic and cathodic peaks are observed. The intensities of the peak currents for the electrodes used depend on the amount of dye loading in the matrices. For SiSb/MB a higher peak current intensity and peak definition were obtained for a dye loading of 14.3 μmol g^{-1} (d/m = 0.8) (Fig. 4d). For electrodes prepared containing the materials with 35.1 μmol g^{-1} (d/m = 1.3) and 3.6 μmol g^{-1} (d/m = 0.5) loadings, a significant decrease in the peak current intensities is observed (Fig. 4b, c). For a lower loading the amount of electroactive species is low and the current is lower, as expected. However, a higher loading should block some electroactive species in the pore of the matrix, decreasing the signal. A diminishing effect of the surface acidity is observed by the E_m values. For this reason, the electrode with a MB loading of 14.3 μmol g^{-1} was used in all further experiments. Similarly, for the SiSb/MeB and SiSb/TB electrodes, matrices having 12.5 μmol g^{-1} (d/m = 1.3) and 22.8 μmol g^{-1} (d/m = 2.3), respectively, were used.

The midpoint potentials for the dyes found on the graphite-modified surface electrodes (against SCE) at solution pH 7 are: (1) MeB, −0.17 [19], (2) MB, −0.27 [17] and (3) TB, −0.3 V vs. SCE [21]. These potentials are influenced by changing the solution pH and normally shift toward more positive values as the pH is lowered. For the dyes adsorbed on SiO_2/Sb_2O_3, such behavior was not observed for the solutions and the midpoint potentials of the adsorbed dyes were shifted toward more positive values and remained constant between pH 3 and 7, i.e. −0.059, −0.17 and −0.18 V vs. SCE for MeB, MB and TB, respectively. Presumably the reduced form of the adsorbed dye is more stabilized inside the matrix pores [38]. Since these dyes are also strongly entrapped inside the matrix pores (they are not leached from the surface at least at pH 2 in 0.5 mol L^{-1} KCl supporting electrolyte solution), they are not affected by the external solution pH change. This behavior cannot be explained by a simple ion exchange adsorption. An interaction of the acid-base type is more convenient to explain such behavior.

An experiment that clearly showed that the dyes are strongly adsorbed inside the matrix pores is the experiment where the anodic current (Ip_a) intensities were checked after several reduction-oxidation cycles. After 300 cycles the peak current intensities remained practically constant for the electrodes, showing that the dyes are not leached out from the matrix surfaces. This is an important aspect since surface dye concentrations remaining constant during various oxidation-reduction operation cycles is a desirable condition for use of these materials as electrochemical sensors.

Plotting Ip_a against the square root of the scan rates (Fig. 5), a linear correlation was obtained in every case ($r = 0.999$), results which are very similar to those observed for diffusion-controlled processes [39]. However, as the electroactive species are strongly immobilized on the matrix surfaces, electrolyte diffusion in and out at the solid/solution interface during the redox process, in order to keep electroneutrality, could explain the observed behavior. The material SiO_2/Sb_2O_3 has a considerably high internal resistance due to the insulator character of silica, and thus an alternative to electron transfer could be an electron hopping mechanism, i.e. electrooxidation of the dye on the surface should occur by a process of an electrooxidized dye molecule oxidizing an adjacent one. The low current observed for lower loading of the dyes could reinforce this suggestion.

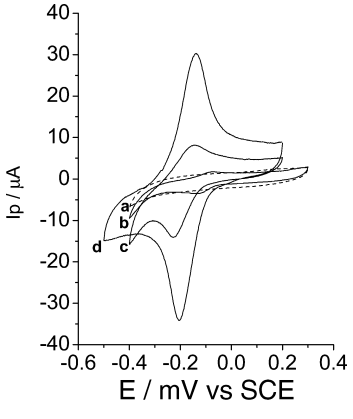

Fig. 4 Cyclic voltammograms obtained for SiSb (*a*) and for SiSb/MB: (*b*) 3.6 μmol g^{-1}, (*c*) 35.1 μmol g^{-1} and (*d*) 14.3 μmol g^{-1}. Measurements in 0.5 mol L^{-1} KCl at a scan rate of 20 mV s^{-1}

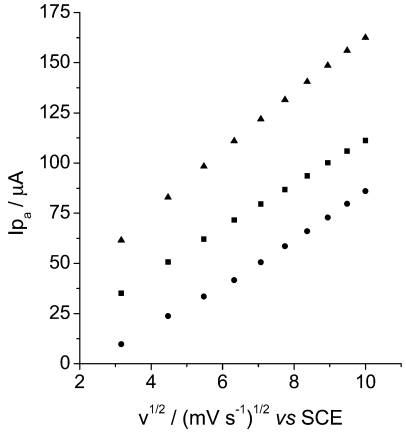

Fig. 5 The cathodic peak current dependence on the scan rate obtained for SiSb/MeB (*squares*), SiSb/MB (*circles*) and SiSb/TB (*triangles*). Measurements in 0.2 mol L^{-1} KCl, pH 6

Electrocatalytic NADH oxidation

The ability of the electrode in catalyzing NADH oxidation was tested for each of the three dyes. The preliminary experiments were carried out by using the cyclic voltammetry technique. Figure 6 shows the electrochemical behavior of the SiSb/MB-modified carbon paste electrode in the presence of NADH at a solution pH of 7. The curves obtained with NADH (Fig. 6B) show that the anodic wave of the mediator increased in comparison with that observed without the coenzyme (Fig. 6A), in a feature similar to that reported for electrocatalytic oxidation of NADH by a similar mediator [40]. Similar results were also obtained for electrodes modified with MeB and TB and, thus, these cyclic voltammetry curves are not presented.

Figure 7 shows the response curves of the SiSb/dye-modified carbon paste electrodes as a function of

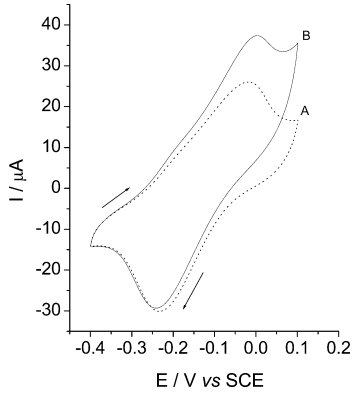

Fig. 6 Cyclic voltammogram curves for SiSb/MB: (*A*) in the absence of NADH and (*B*) in the presence of 10 mmol L^{-1} NADH. Measurements in 0.06 mol L^{-1} KCl/0.2 mol L^{-1} phosphate buffer solution, pH 7, at a scan rate of 20 mV s^{-1}

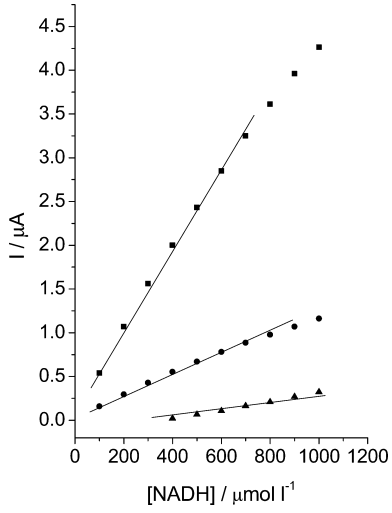

Fig. 7 Calibration plot for NADH obtained with carbon paste electrodes modified with SiSbMeB (*squares*), SiSb/MB (*circles*) and SiSb/TB (*triangles*) in 0.06 mol L^{-1} KCl/0.2 mol L^{-1} phosphate buffer solution, pH 7, at an applied potential of 0 mV vs. SCE

Table 2 NADH electrooxidation using the organic dyes immobilized onto SiSb. Experiments carried out in 0.2 mol L^{-1} KCl/0.06 mol L^{-1} phosphate buffer solutions

SiSb/dye	E_m (mV)	LR[a] (mmol L^{-1})	S[b] (mA L mol^{-1})	DL[c] (μmol L^{-1})
SiSb/MeB	−76	0.1–0.6	4.6	7
SiSb/MB	−124	0.1–0.6	1.8	25
SiSb/TB	−141	0.4–1	0.5	42

[a]LR = linear response range
[b]S = sensitivity
[c]DL = detection limit

NADH concentration. The data were obtained from chronoamperometric experiments, where the potential was fixed at 0 mV vs. SCE, to electrocatalyze all NADH present on the surface of the electrode. Among the mediators studied, MeB, with a higher E_m, showed better electrocatalytic activity in terms of current for NADH oxidation. Among the phenoxazine mediators studied earlier [41], the faster reaction was with immobilized MeB. The linear response range was the same for SiSb/MeB and SiSb/MB, but the former gave higher sensitivity and a lower detection limit. The detection limit was determined considering a signal-to-noise ratio equal to three. The parameters obtained for the each dye immobilized onto SiSb for NADH electrooxidation are presented in Table 2.

Conclusions

Some organic dyes (MeB, MB and TB) were immobilized into SiSb prepared by the sol-gel processing method. Carbon paste modified with this material, having dyes immobilized on its surface, showed high chemical stabilities, assigned to the strong adsorption of the dyes on the matrix. When the monomeric species is predominant, the acidity of the matrix is more pronounced, as could be observed by the E_m value. The resulting SiSb/dye-modified electrodes exhibit electrocatalytic ability of differing degrees for NADH oxidation. The shift in the formal potential of the immobilized organic dyes toward more positive values and its invariance with solution pH make SiSb/MeB an interesting material for biosensor development, coupled to a dehydrogenase enzyme.

Acknowledgements E.S.R. and S.S.R. are indebted to the Fundação de Amparo à Pesquisa do Estado de São Paulo (FAPESP), Brazil, for post-doctoral and PhD fellowships, respectively. Y.G. and L.T.K. acknowledge FAPESP and FINEP/Pronex for financial support. The authors thankl Prof. Carol H. Collins for English language revision.

References

1. Alfaya AAS, Gushikem Y (1999) J Colloid Interface Sci 209:428–434

2. Zaitseva G, Gushikem Y, Ribeiro ES, Rosatto SS (2002) Electrochim Acta 47:1469–1474
3. Gao XT, Fierro JLG, Wachs IE (1999) Langmuir 15:3169–3178
4. Menon V, Popa VT, Contescu C, Schwarz JA (1998) Rev Roum Chim 43:393–397
5. Miller JM, Lakshmi LJ (1998) J Phys Chem B 102:6465–6470
6. Kochkar H, Figueras F (1997) J Catal 171:420–430
7. Dutoit DCM, Schneider M, Fabrizioli P, Baiker A (1997) J Mater Chem 7:271–278
8. Castellani AM, Gushikem Y (2000) J Colloid Interface Sci 230:195–199
9. Gonçalves JE, Gushikem Y, de Castro SC (1999) J Non-Cryst Solids 260:125-131
10. Walcarius A (1998) Electroanalysis 10:1217–1235
11. Walcarius A (2001) Chem Mater 13:3351–3372
12. Walcarius A (2001) Electroanalysis 13:701–718
13. Ferreira CU, Gushikem Y, Kubota LT (2000) J Solid State Electrochem 4:298–303
14. Kubota LT, Gouveia F, Andrade AN, Milagres BG, Oliveira Neto G (1996) Electrochim Acta 41:1465–1469
15. Perez EF, Oliveira Neto G, Kubota LT (2001) Sens Actuators B 72:80–85
16. Pessoa CA, Gushikem Y, Kubota LT (1997) Electroanalysis 9:800–803
17. Pessoa CA, Gushikem Y, Kubota LT, Gorton L (1997) J Electroanal Chem 431:23–27
18. Ottaway JM (1972) In: Bard AJ (ed) Indicators. Pergamon, Oxford, pp 469–529
19. Gorton L, Tortensson A, Jaegfeldt H, Johansson G (1984) J Electroanal Chem 161:103–120
20. Chi Q, Dong S (1995) Electroanalysis 7:147–153
21. Malinauskas A, Ruzgas T, Gorton L (2000) J Electroanal Chem 484:55–63
22. Galip H, Hasipoglu H, Gunduz G (1999) J Appl Polym Sci 74:2906–2910
23. Sato H, Kondo K, Tsuge S, Ohtani H, Sato N (1998) Polym Degrad Stabil 62:41–48
24. Jung HC, Kim WN, Lee CR, Suh KS, Kim SR (1998) J Polym Eng 18:115–130
25. Carty P, White S (1995) Polym Degrad Stabil 47:305–310
26. Nalin M, Poulain M, Ribeiro SJL, Messaddeq Y (20001) J Non-Cryst Solids 284:110–116
27. Schubert UA, Anderle F, Spengler J, Zuhlke J, Eberle HJ, Grasselli RK, Knozinger H (2001) Top Catal 15:195–200
28. Youk JH, Kambour RP, MacKnight WJ (2000) Macromolecules 33:3606–3610
29. Zanthoff HF, Grünert W, Buchholz S, Heber M, Stievano L, Wagner FE, Wolf GU (2000) J Mol Catal A 162:435–454
30. Vislovskiv VP, Bychkov VY, Sinev MY, Shamilov NT, Ruiz P, Schay Z (2000) Catal Today 61:325–331
31. Janardanan C, Nair SMK (1992) Indian J Chem A 31:136–138
32. Janardanan C, Nair SMK (1990) Analyst 115:85–87
33. Goodhew PJ, Humphreys FJ (1992) Electron microscopy and analysis, 2nd edn. Taylor & Francis, London, pp 154–198
34. Bearden JA (1967) Rev Mod Phys 39:78–124
35. Antonov L, Gergov G, Petrov V, Kubista M, Nygren J (1999) Talanta 49:99–106
36. Jockusch S, Turro NJ, Tomalia DA (1995) Macromolecules 28:7416–7418
37. Schlereth DD, Karyakin AA (1995) J Electroanal Chem 395:221–232
38. Munteanu FD, Kubota LT, Gorton L (2001) J Electroanal Chem 509:2–10
39. Bard AJ, Faulkner LR (1980) Electrochemical methods: fundamentals and applications. Wiley, New York, pp 519–540
40. Persson B, Gorton L (1990) J Electroanal Chem 292:115–138
41. Kubota LT, Munteanu F, Roddick-Lanzilotta A, McQuillan AJ, Gorton L (2000) Quim Anal 19:15–27